

Hyaluronic Acid-Alginate Based Augmentation in Peripheral Nerve Repair: Histologic Landscape and Proteomic Profiling

Amit S. Mohite¹, Crystal Jing¹, Marcus Valenta², Meredith Cox¹, Christian Zirbes¹, Neill Li³

¹Department of Orthopaedic Surgery, Duke University School of Medicine, Durham, NC,

²Molecular Genetics and Microbiology, Duke University School of Medicine, Durham, NC

³Department of Neurosurgery, Duke University School of Medicine, Durham, NC

amit.mohite@duke.edu

Disclosures: Amit Mohite(N), Crystal Jing(N), Meredith Cox(N), Marcus Valenta(N), Christian Zirbes(N), Neill Li(N)

INTRODUCTION: Biomaterial supplementation intraoperatively has shown elucidating support for the mechanisms of peripheral nerve regeneration, garnering interest by aiding the modulation of extracellular matrix inflammatory microenvironments, reducing scar tissue formation, and providing mechanical guidance for biologies to stabilize structural healing. Hyaluronic acid (HA) has demonstrated ameliorating benefits to wound healing across multifactorial disciplines in medicine, but has limited evidence on its effect on the conditions of regeneration after nerve repair. Alginate crosslinked with calcium in corresponding concentrations allows for the phase separation of HA creating a percolation network possibly promoting neuronal and cellular projection and migration. This preclinical study aims to characterize neuroregenerative cellular responses and molecular regulation of sciatic nerves within an injury/repair rodent model with and without the use of a commercially available hyaluronic acid/alginate hydrogel at the critical 14 day post-surgical marker. By doing so, our goal is to provide a rigorous scientific evaluation for the clinical use of HA in peripheral nerve reconstruction surgeries.

METHODS: Six-month old C57BL/6 male mice were randomized into HA/alginate-treated and untreated groups. Mice underwent a full transection on both hind limbs 6mm from the trifurcation site with microscissors, a microsurgical repair was then done under a Zeiss Stemi 2000-C light microscope with a single 10-0 nylon suture. Mice were treated with the application of 50 μ L of HA/alginate-based hydrogel at the coaptation site on the right side, the left side remained untreated without hydrogel treatment. Both surgical sites were closed with 5-0 nylon suture. Fourteen days postoperatively, sciatic nerves were carefully dissected. Sciatic nerve tissue used for histology were fixed in PFA 4% PBS after dissection, dehydrated with 30% sucrose, embedded in OCT flash frozen in dry ice and sectioned at 10 μ m on a Leica cryostat. Optimal tissue sections were used approximately 100-200 μ m into the cryoblock. Sections with minimal nylon suture artifact were stained with axon NF-L, macrophage F4/80, Schwann cell S100B, Endothelial cell CD31, Fibroblast NKK-66 antibodies. DAPI mounting media was applied after immunofluorescent staining to highlight nuclei. Coaptation site was imaged on a Leica ZM5600 fluorescent microscope. Quantification of fluorescent signals were calculated by Fuji ImageJ software. Sciatic nerve tissue used for proteomic profiling were frozen down with liquid nitrogen and processed for mass spectrometry on the Orbitrap Fusion Lumos. Nerves were dissociated with SDS into their peptide constituents. Peptides were further processed for liquid chromatography column gradients. Data-dependent acquisition was done for a resolution of 60,000 at m/z 200. MaxQuant was used for bioinformatic analysis missing data was imputed and normalized, significantly regulated proteins were found with $\log_2FC > 2$, $FDR < 0.01$ before performing gene ontology analysis. 3 mice were used for histological analysis, 3 mice were used for proteomic analysis.

RESULTS: Immunofluorescent imaging at the coaptation site presents successful Schwann cell and axonal bridging structures past the site of repair 14 days post operation in both HA treated and primary repair untreated nerves. NF-L staining fill% quantified 10.7% recovery in Hyaluronic Acid treated nerves and 8.42% in Primary Repair untreated nerves. Schwann cell matriculation at the repair site revealed 23.1% bridging fill% for Hyaluronic Acid treated nerves and 18.2% Primary Repair untreated nerves. Macrophage, Endothelial cell, and Fibroblast counts respectively quantified 512, 943, 734 counts for HA supplemented nerves and 572, 724, 859 counts for primary repair nerves. Proteomic profiling identified the upregulation of genes *Agtr2*, *Tusc1*, and *Aqp2* and the downregulation of *Timp4*, in a HA treated compared to untreated suggesting the activation of transcribed proteins seen in the volcano plot possibly correspond to the observed cluster of significant protein expression. Gene Ontology Enrichment characterized these molecular factors to reparative processes including DNA repair, chromatin remodeling, and cell cycle reactivation.

DISCUSSION: The cellular diffusion demonstrated progressing through the repair site shown in the histology evaluates the infiltration of regenerative cells actively migrating ahead of the regenerating axons to assist in myelination and the remodeling of the restorative environment. The density of macrophages, endothelial cells, and fibroblasts indicates both groups treated and untreated have successful propagation of cellular colocalization necessary for axonal maturation. Migratory patterns response distally from the coaptation site staggered near the suture indentation in both groups but had larger discrepancies in the untreated primary repair sections. *Agtr2*, *Tusc1*, and *Aqp2* genes highlighted in the proteomic analysis contribute to membrane ion regulation facilitating cell survival and enhanced metabolic activity possibly yielding to the robust molecular support of cellular function within HA treated nerves. Proteomic downregulation of fibrosis-associated proteins such as *Col26a1* and *Thbs2* further indicates suppression of matrix stiffening, allowing improved cell motility across the repair junction alluding to the advantageous role HA may have compared to primary repair. Collectively, this data suggests the proteomic shifts are tightly coordinated with histological observations, where reduced scarring and enhanced metabolic signaling coincide with cellular integration at the coaptation site following HA/Alginate application.

SIGNIFICANCE/CLINICAL RELEVANCE: This study indicated axonal recovery is not inhibited by the implantation of hyaluronic acid alginate hydrogel by using a clinically relevant repair model. Our data substantiates predominant molecular factors succeed in captivating peripheral nerve regeneration in HA/Alginate treated nerves compared to primary repair nerves in the absence of biomaterial augmentation.

ACKNOWLEDGEMENTS: Funding support provided by Alafair Biosciences

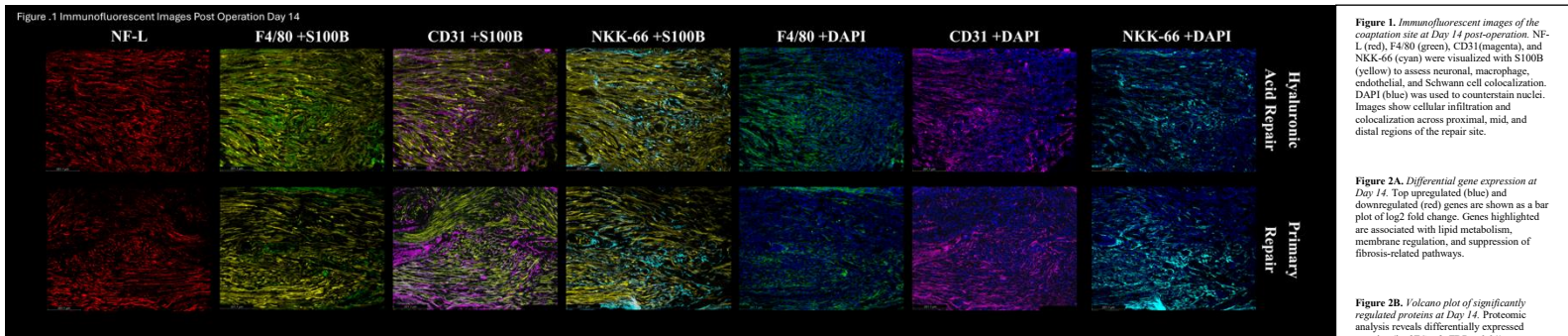


Figure 1. Immunofluorescent images of the coaptation site at Day 14 post-operation. NF-L (red), F4/80 (green), CD31 (magenta), and NKK-66 (cyan) were visualized with S100B (yellow) to assess neuronal, macrophage, endothelial, and Schwann cell colocalization. DAPI (blue) was used to counterstain nuclei. Images show cellular infiltration and colocalization across proximal, mid, and distal regions of the repair site.

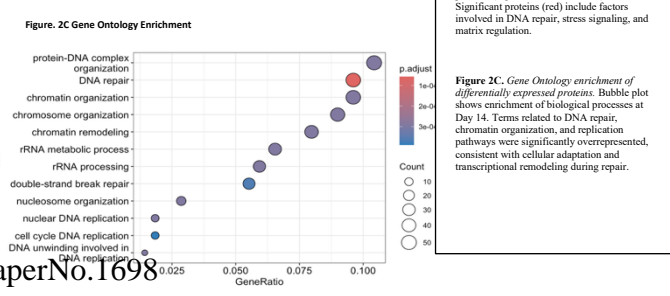
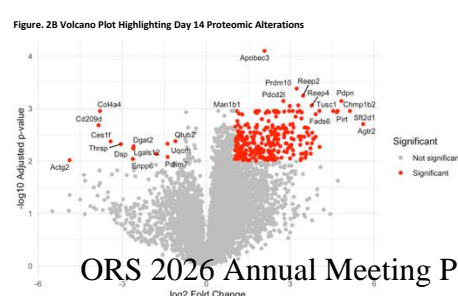
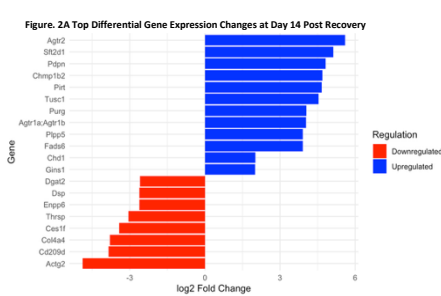


Figure 2A. Differential gene expression at Day 14. Top upregulated (blue) and downregulated (red) genes are shown as a bar plot of \log_2 fold change. Genes highlighted are associated with lipid metabolism, membrane regulation, and suppression of fibrosis-related pathways.

Figure 2B. Volcano plot of significantly regulated proteins at Day 14. Proteomic analysis reveals differentially expressed proteins ($\log_2FC > 2$, $FDR < 0.01$). Significant proteins (red) include factors involved in DNA repair, stress signaling, and matrix regulation.

Figure 2C. Gene Ontology enrichment of differentially expressed proteins. Bubble plot shows enrichment of biological processes at Day 14. Terms related to DNA repair, chromatin organization, and replication pathways were significantly overrepresented, consistent with cellular adaptation and transcriptional remodeling during repair.